NCG-NACL RESERVOIR MODELLING IN WAIOTAPU-WAIKITE-REPOROA GEOTHERMAL AREAS

Eko Hari Purwanto [1] and Eylem Kaya [2]

[1] Directorate of Geothermal, Ministry of Energy and Mineral Resources, Indonesia

[2] Department of Engineering Science, University of Auckland, New Zealand

e.kaya@auckland.ac.nz

Keywords: *Waiotapu, Waikite, Reporoa, EWASG, heat discharge, geothermal reservoir modeling*

ABSTRACT

Natural state simulation of the Waiotapu, Waikite and Reporoa geothermal fields was previously carried out, with a saturated atmosphere model, by Kaya *et al.* (2014). In the present study, the model is modified so that the effects of saline fluids (NaCl) and non-condensable gases (NCG), on the Great Waiotapu system, can be considered. The previous saturated zone model is extended to include a gas/water interface. This enables the unsaturated zone, close to the ground surface, to be included in the model, and also increases the ability of the model to represent the infiltration zones. Additional surface manifestations are considered (i.e. surface heat discharges from Maungakakaramea and Maungaongaonga) for a more accurate representation of the Waiotapu region. The model is recalibrated in order to achieve agreement with available natural state downhole temperature data, magnitudes and locations of heat flow to the surface, as well as, measured chloride data.

For the best fit model, the quantity of total mass upflow was assigned to be approximately 720 kg/s, which includes NaCl content ranging from 0.04 to 0.32% and CO_2 content of 0.024%. The result of this model gives a total heat loss of ~685 MW and estimates Cl flux across the system to be 244 g/s.

1. INTRODUCTION

Waiotapu, Waikite and Reporoa geothermal fields (WWR) are located along the eastern side of the Taupo Volcanic Zone (TVZ). These three thermal areas lie in close proximity to each other and have been subject to several studies, particularly regarding the possible connections that may exist between them (e.g. Bibby *et al.*, 1994; Healy & Hochstein, 1973; Wood, 1994).

The region that includes the WWR fields is featured by the Reporoa Caldera in the South, by SW–NE trending structural features, such as the Paeroa Fault Zone and the Ngapuri Fault, in the west, and by the Kaingaroa Plateau in the eastern hills. The Reporoa Caldera was redefined by Nairn *et al.* (1994) as a collapse-caldera with residual magma bodies underneath, which could act as a heat source for the hydrothermal activity associated with the caldera. The Reporoa Caldera is a single, sub-circular caldera, with a surface area of 11 x 13 km and with the lower elevation side of the caldera facing to the south. Subsurface geological information retrieved from exploratory wells and previous geological mapping informs that the WWR areas are comprised of laterally extensive pyroclastic layers with minor andesites, rhyolite and dacite (Grindley *et al.*, 1994).

The Waiotapu geothermal field, located at the northern end of the Reporoa Caldera, is the largest of the 20 major geothermal areas in the TVZ having the extent of 17 km^2 of active manifestations. Initially, exploratory drilling campaigns between 1956 and 1959, at seven sites, were held across the thermal area and successfully obtained high temperature measurements of up to 295^{o}C (Hedenquist & Browne, 1989). Surface thermal manifestations consisted of acid-sulphate mud pools, thermal lakes, steaming ground, minor fumarolic activities and thermal springs. Geological, geophysical, and geochemical studies have been reported through a series of articles in the 1994 *Geothermics* journal (Geothermics, 1994).

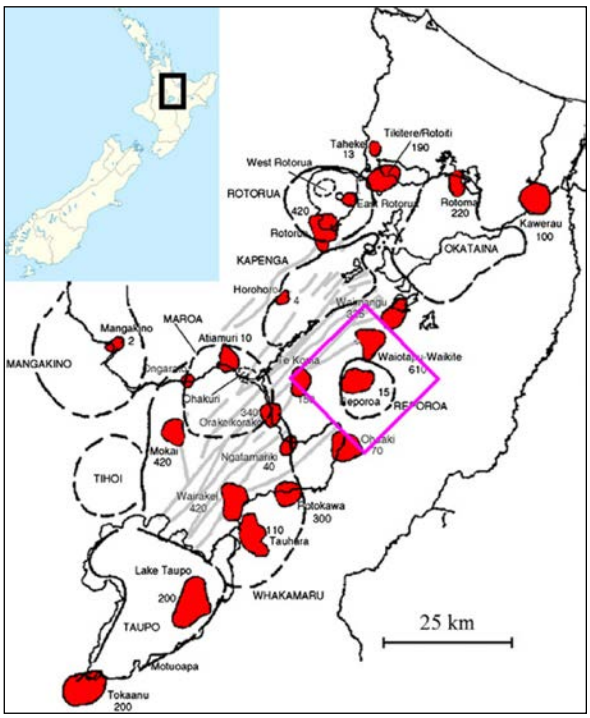

Figure 1. Location of WWR fields (in pink rectangle) (Kaya et al. 2014)

The Reporoa geothermal field is located inside the Reporoa Caldera boundary and approximately 7 km to the south of the Waiotapu area. Wood (1994) interpreted that collapsed structures of the Reporoa Caldera may have originated reservoir permeability in the Waiotapu-Reporoa geothermal system. Considerable thermal activity beneath the Reporoa area is shown by the low resistivity anomaly of <10 Ωm (Bibby *et al.*, 1994), which indicates an area of concealed thermally altered rocks of approximately 10 km^2. Thermal activities in Reporoa are characterized by hot pools, thermal ground, fumaroles and thermal springs. In 1966, well RP1 was drilled near hot springs in the center of the Reporoa caldera to a depth of 1338 m. A maximum temperature of 255 ^{o}C was measured in 975 m. Conversely, temperature inversion occurred between 400 to 670 m, caused by cold water influx (Bignall, 1990).

The Waikite geothermal field lies about 5 km from the west of the Waiotapu thermal area and is separated by the elevated Paeroa range. It lies within the Paeroa fault depression where hot spring discharge is controlled by downthrown blocks on the side of the Paeroa scarps (Wood, 1994). The interpretation of resistivity measurements suggest that the Waikite and Waiotapu systems share an area underneath the Paeroa blocks which consist of a low resistivity zone value of < 20 Ωm (Bibby *et al.*, 1994). An estimation of 43 MW total heat flow was observed from waters draining to the valley (Glover *et al.*, 1992).

Based on published geological, geophysical, and geochemical surveys and using some recently measured field data, Kaya *et al.* (2014) set up a numerical model in order to investigate the underground movement of hot and cold flows, which elucidates the gross permeability distribution within the region. Kaya *et al.* (2014) only considered a water (liquid and vapour) component. This meant that the unsaturated region close to the ground surface was not modelled and the effect of geochemical substances was not included. The model discussed, in this paper, uses the model developed by Kaya *et al.* (2014), as a base model. In order to represent shallow zones more accurately and include changes to the surface features, the top of the model was modified to follow the surface topography and the model required a further refined grid, in vertical directions. The use of the CO_2-water and the NCG- NaCl equation of states enable the unsaturated zone close to the ground surface to be included in the model. The model is calibrated against more observational data (i.e. additional surface heat discharge and Cl surface flux data), in addition to the observational data used by Kaya *et al.* (2014) (i.e temperature profiles, surface heat loss measurements). With the addition of these details, the model aims to provide a more accurate representation of the natural state conditions, in order to obtain a better understanding of the underground mass and heat flow reservoir behaviour.

2. GEOCHEMISTRY

Since 1937, several chemical surveys have been conducted to provide a general guide for determining a conceptual model that consists of an upflow zone and fluid flow paths of WWR fields. One of the most comprehensive geochemistry reports on WWR fields was provided by Giggenbach *et al.* (1994). A series of samples from hot springs, pools and streams was analyzed and plotted on a Cl-SO_4-HCO_3 diagram, as seen in Figure 2.

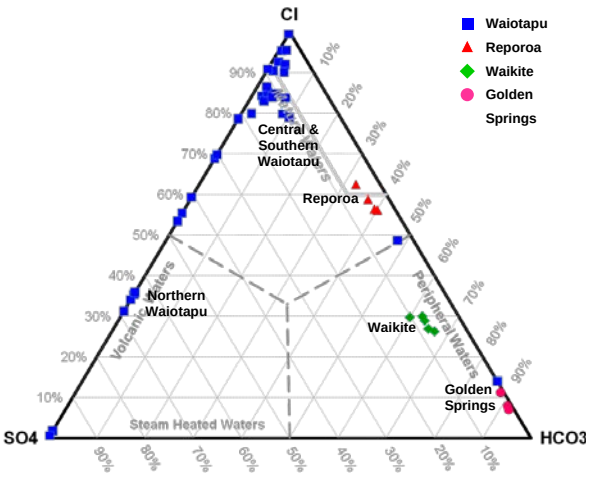

Figure 2. Cl-SO4-HCO3 ternary plot based on data modified from Giggenbach *et al.* (1994)

Geochemical interpretation from the plot indicates that the main upflow, of high temperature water, in Waiotapu, occurs in central and southern Waiotapu, with additional heat input from beneath Reporoa. Giggenbach *et al.* (1994) indicate that the heat source is located near the base of two dacite domes, in northern area, with neutral Cl water flows, to the south, through Champagne Pool. The Champagne Pool discharges the highest concentration of chloride (from 1600 mg/kg to more than 2200 mg/kg), whereas the average CO_2 content is considered low, 240 mg/kg.

Secondary deep inflow that feeds the southern area in Reporoa is characterized by Cl-HCO_3 waters, with shallow dilution from Waiotapu. Southern low temperature manifestations in the south of Reporoa (Golden Springs and Butcher's Pool) with high HCO_3 content indicate that peripheral water originated from a lower temperature envelope of high Cl water (Giggenbach *et al.*, 1994). HCO_3 concentration and high isotopic composition of deeper volatile species (CO_2 and CH_4) indicate deep, high-temperature fields beneath both Waiotapu and Reporoa. It is also likely that outflow from Waiotapu and deeper volatile upflow beneath Reporoa (Hochstein, 2007) together contribute to the formation of the Reporoa field.

The Waikite geochemical spring samples, in Figure 2 plotted in green dots close to the HCO_3 apex, show a high HCO_3/Cl ratio. This indicates that shallow-peripheral water is formed at the margin of the major upflow zone. Surface deposition of calcium carbonate (travertine) is also deposited, which is uncommon for natural discharge in the TVZ, and is indicative of a margin area of a high temperature upflow zone (Hochstein & Browne, 2000).

Areal distribution of surface Cl concentration is given in Figure 3. Surface discharge of pools and streams and data obtained from wells given in Giggenbach *et al.* (1994) are used to plot this contour map.

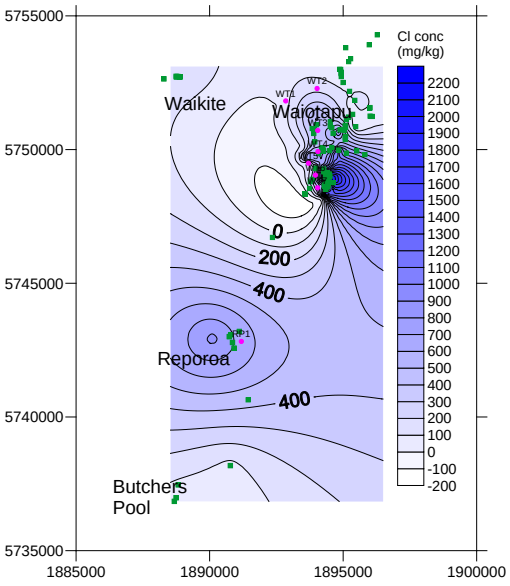

Figure 3. Surface chloride concentration distribution map based on data from Giggenbach *et al.* (1994)

Figure 3 illustrates that the both the Waiotapu and Reporoa areas have significant concentrations of Cl. As it is also shown in the ternary plot, shown in Figure 2, this Cl distribution map indicates that either similar spring compositions occur in Waiotapu and Reporoa by different

processes or that similar processes operate in different areas (Pope & Brown, 2014).

The geochemical interpretation of the hydrothermally altered zone is coherent with the low resistivity signature between Reporoa and Waiotapu which interpreted an additional independent, deep upflow beneath Reporoa (Bibby *et al.*, 1994), as seen in Figure 4.

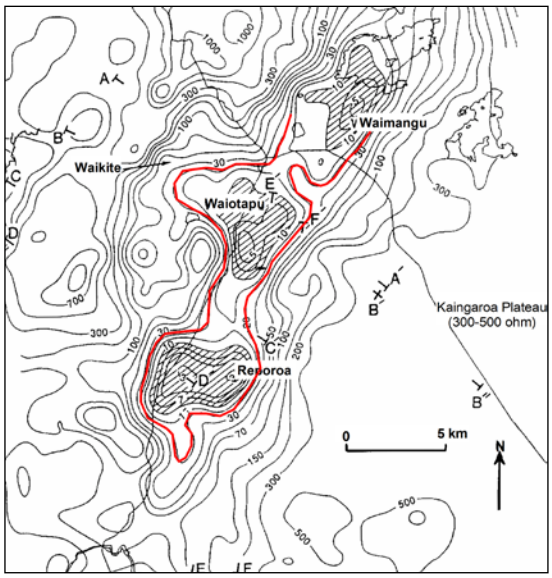

Figure 4. Resistivity boundary encompassing WWR fields modified from Risk *et al.* (1994). Red line indicates 20 Ωm

3. HEAT MEASUREMENTS

Heat discharges from thermal areas are mainly defined by the following mechanisms: 1) Conduction, diffusion and radiation from bare ground, 2) Evaporation and radiation from water surfaces, 3) Advection from fumaroles and hot springs.

Direct method is one of the methods to assess the heat loss (Sorey and Colvard, 1994). This method considers advective heat loss from steam vents (H_{FUM}), advective heat loss of streams and springs (H_{ADV}), evaporative heat loss from water surface (H_{EVAP}), radiative heat loss from the surface of the water (H_{RAD}), conductive and diffusive heat loss from water surfaces (H_{COND}), and heat loss from bare ground by convection, evaporation & conduction (H_{GR}) as given in Equation (1). Parameters such as atmospheric pressures, mean wind speed, temperatures of streams, pools and steam vents; and flow rates of streams and steam vents are also included in this method.

$$H_{TOT} = H_{FUM} + H_{ADV} + H_{EVAP} + H_{RAD} + H_{COND} + H_{GR} \quad (1)$$

Smith (2013) used a similar approach in order to assess the heat loss distribution in WWR areas by using surface heat flow measurements for estimating total heat discharges from the Waiotapu geothermal areas in 2013. An ambient temperature of 12°C was selected (which reflects a slightly warmer temperature at 330 masl) and an average wind speed of 3 m/s (which fits a 30 year mean wind speed in the central TVZ). For Waikite, Reporoa, Golden Springs and Butcher's Pool, surface temperature and mass flow rate data were gathered from annual surface thermal feature monitoring by Lynne (2009), Newson (2010), Littler (2012), and Wildland Consultants (2001). Surface heat loss estimation was then calculated in the form of advective spring heat loss (anomalous) Q_{ADV} in the following formula:

$$Q_{ADV} = 0.001 \times \dot{m} \times (H_w - H_o) \quad (2)$$

Where m is the mass flow of heated water, H_w is its discharging enthalpy and H_o is the enthalpy of water at reference temperature/ambient temperature. The distribution of surface manifestations can be seen in Figure 5. Heat discharge data used in this study is a summation of measured heat flows as shown in Table 1.

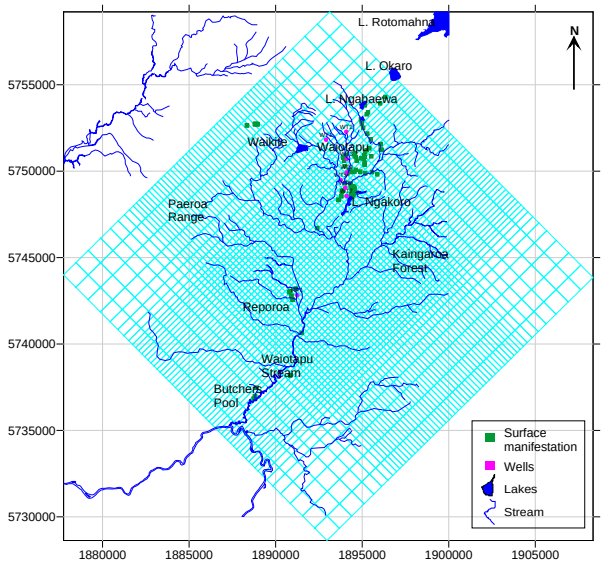

Figure 5. Distribution of surface manifestations within WWR areas

Table 1. WWR heat flow summary

Field		Q (MW)	Remark	Reference
Waiotapu (581 MW)	Water Surface	423	Q_{EVAP}, Q_{RAD}, and Q_{COND}	Smith (2013)
	Steaming Ground	130	Q_{FUM}	Benseman *et al.* (1963)
	Hot Spring	28	Q_{ADV} of spring *	Lynne (2009), Newson (2010), Littler (2012)
Waikite		50	Q_{ADV} of spring *	Lynne (2009), Newson (2010), Littler (2012)
Reporoa		36	Q_{ADV}, Q_{EVAP}, Q_{FUM}	Hochstein (2007)
Golden Springs -Butcher's Pool		14	Q_{ADV} of spring *	Wildland Consultants (2001)

* calculated from monitoring reports

Measured heat discharges from each surface manifestation were used to plot the heat flow contours, shown in Figure 6. This figure shows that the Waiotapu area has the highest heat discharge.

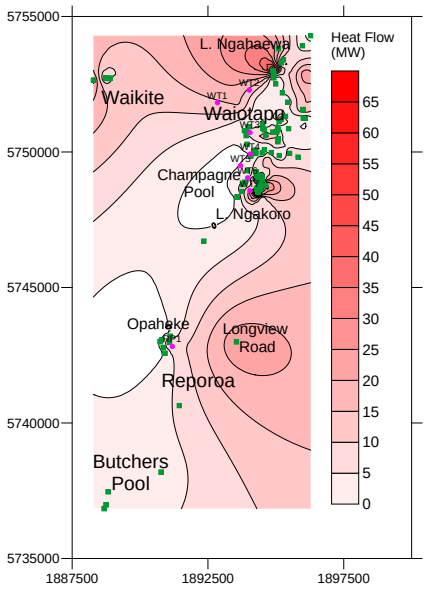

Figure 6. Surface heat loss contour map (plotted by using data from (Littler, 2012; Lynne, 2009; Newson, 2010; Smith, 2013; Wildland Consultants, 2001)

It can be inferred from the map that the areas, including Lake Ngahewa (22 MW) and Lake Rotowhero (58 MW), in the northern area of Waiotapu have high amounts of heat flow to the surface. Another concentrated heat flow area is located at southern part of Waiotapu, where the Champagne Pool (43 MW), Lake Whangioterangi/Echo Lake (39 MW) and Lake Ngakoro (82 MW) are situated. There is additional surface heat discharged (i.e ~100 MW total discharge from Maungakakaramea and Maungaongaonga estimated by Hochstein (2014)) but these discharge values were not represented in Figure 6.

4. CONCEPTUAL MODEL

Several important data (i.e. lithological features, temperature profiles, fluid chemistry, heat discharge) were gathered to describe the conceptual model of the system. According to Giggenbach *et al.* (1994), the main feedzone underneath Waiotapu is located at shallow depth of -400 mRL (Figure 7). The maximum measured temperature at 1000 m is 295°C (Hedenquist & Browne, 1989) and reservoir fluid carries out ~1350 mg/kg neutral Cl, as observed in Champagne Pool (Hedenquist, 1991). The neutral Cl waters at other adjacent springs at margin of the system have been diluted by CO_2-rich steam heated water.

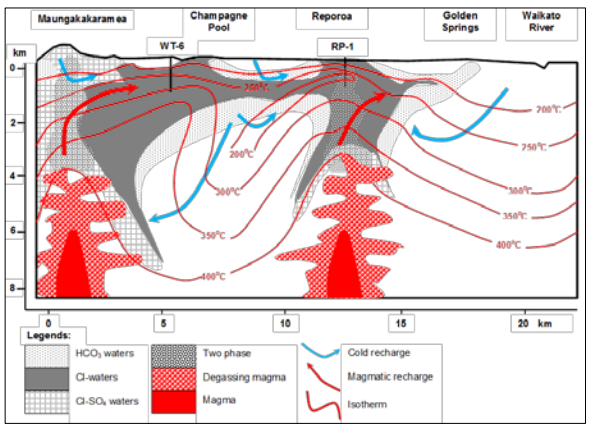

Figure 7. Hydrothermal system based on fluid and gas geochemistry modified from Giggenbach *et al.* (1994)

Additional upflow for Reporoa provides ~800 mg/kg Cl flow, which comes from different high temperature parent waters. The ascending waters are diluted by the southward flow of 150°C condensate (Giggenbach *et al.*, 1994).

Waikite, in this system, is considered as an outflow area, where the Paeroa fault zone acts as a westward conduit that transfers geothermal water upward from a shallow aquifer in Waiotapu (Wood, 1994).

The hydrological pattern of WWR fields is also influenced by cold groundwater inflow fluid from both the Kaingaroa and the Paeroa depression and by infiltration from above Ngapouri Flat and northern dacite domes in the north and Opaheke in the south, as shown in Figure 8.

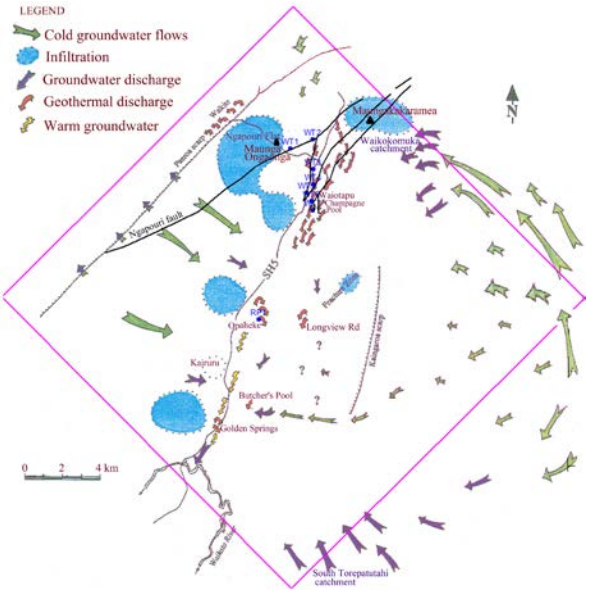

Figure 8. Hydrology of the WWR system, modified from Newson (1993)

5. COMPUTER MODEL

A large scale numerical model (named WWR-1) was set up by Kaya *et al.* (2014) to represent WWR fields. WWR-1 was built to test various conceptual models. The reservoir fluid is treated as pure water hence the EOS 1 module of AUTOUGH2 (Yeh *et al.*, 2012; O'Sullivan *et al.*, 2013), The University of Auckland version of TOUGH2 (Pruess *et al.*, 1999), was used, to calibrate that model. WWR-1 covers an area of 450 km^2 with a rectangular grid of 57 x 57 horizontal blocks, which results in a total of 3,249 columns. It contains 16 layers, with a total of 51,426 blocks. WWR-1 extends from an elevation of 500 mRL (sea level is 0 mRL) to -3,000 mRL, so that it is deep enough to represent the Greywacke Basement. WWR-1 gives a good overall match to natural state of the field.

In order to provide a more detailed representation of natural state condition of WWR areas, the WWR-1 model was modified (the new model was named WWR-2). The surface of the WWR-1 model was set at the water table. To represent the unsaturated zone, close to ground surface, and heat and mass flow condition in the shallow zones, surface topography (http://www.linz.govt.nz/topography/topo-maps/) was implemented into the topmost boundary of WWR-2 (Figure 9). Instead of a wet atmosphere a high NCG saturation content was considered at surface conditions and infiltration of rainwater was implemented by injecting a proportion of the average rainfall into the surface blocks.

The effect of NCG and NaCl components was also investigated. EOS2 and EWASG modules of TOUGH2 were used for calibration of WWR-2. The first one enables the unsaturated zone close to the ground surface to be represented in the model, and the latter allows NCG and NaCl components to be included in the simulations. PyTough (Wellmann *et al.*, 2012), Mulgraph (O'Sullivan & Bullivant, 1995) and TIM (Yeh *et al.*, 2013) were used for visualization and data processing. A more refined grid in vertical directions (75 m thick) was used in the shallow levels of WWR-2 model, to give a better accuracy. Vertical layer comparison is presented in Figure 10.

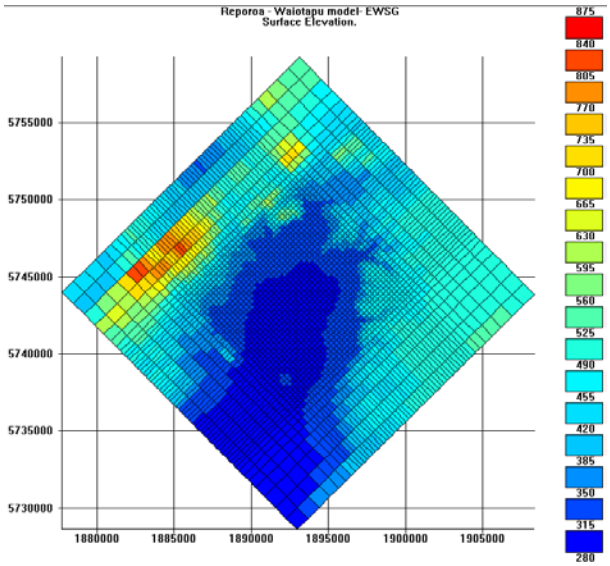

Figure 9. Topography for each model column for WWR-2 Model

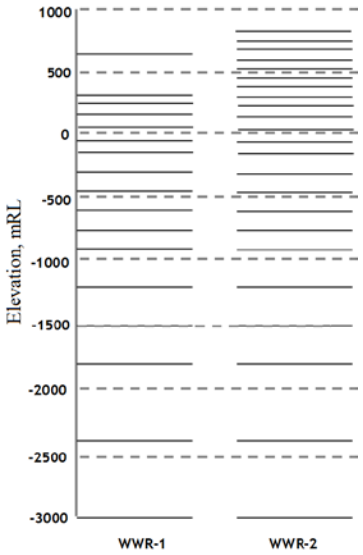

Figure 10. Vertical layer structures for WWR-1 and WWR-2

The EWASG fluid property module was developed by Battistelli *et al.* (1997) and is used primarily for modelling geothermal reservoirs with saline fluids and NCG. EWASG is able to describe liquid and gas phases. This also allows representation of temperature-dependent solubility constraints, due to precipitation and dissolution of salt (NaCl). Thus, variation of chemical concentration can provide information with regard to fluid flow patterns in reservoirs, upflow zone locations, mixing with colder fluids, and boiling/condensation processes in different reservoir zones. Integrating chloride into the model can explain that chloride will increase as boiling takes place and will be diluted when mixing occurs. Summary of the model involved in this paper is presented in Table 2.

Rock properties, in model WWR-2, were initially assumed to be uniform, within a single unit, and were supposed to be similar to WWR-1. All rock types were assumed to have a rock density of 2500 kg/m^3, a thermal conductivity of 2.5 W/m.K, and a specific heat of 1000 J/kg.K (Kaya *et al.*, 2014).

Table 2. Summary of model parameters

Category	WWR-1	WWR-2
Grid area	450 km^2	450 km^2
Grid depth	3,000 m	3,000 m
Number of blocks	51,426	54,216
Surface Temp.	15 ^{o}C	12 ^{o}C
Rainfall rate	-	1,000 mm/year
Infiltration rate	-	10%
Number of layers	16	22
Surface	Water table	Topography
Equation of state	EOS1	EOS2 and EWASG

EOS2 version of AUTOUGH2 was used in order to implement the topography of the region into the model and create an "initial condition" file to modify the primary variables from EOS2 to EWASG. The chemical composition of Na and Cl from surface thermal features along the field was taken into account. An NaCl constituent, which varies from 840 mg/kg to 3200 mg/kg and a CO_2 constituent of 240 mg/kg (Giggenbach *et al.*, 1994; Pope & Brown, 2014) were included as part of the mass fraction in heat and mass input from the basement of the model.

The areas of high surface activity are represented as "spring wells" feeding from model blocks located underneath the caprock (layer 12). The thermal features given in Kaya et al. (2014) and additional heat discharge from Maungaonga (~50MW) and Maungakakaramea (~50 MW) were taken into consideration.

The model was run until steady state conditions were achieved. Shallow permeabilities, location and magnitude of mass and heat inputs, and infiltration rate at the surface conditions were modified manually during calibration.

6. RESULTS

6.1 Heat discharge

The heat discharge distribution of the model, associated with the natural state conditions of the convective and advective fluid flow in the three fields, has been calibrated by varying fluid and heat input at its base and by varying the permeability structure. Then, the total heat discharge to the surface was calculated by the summation of heat flow from the spring wells and heat discharge from the uppermost model layer. Table 3 shows comparison between the model results and the field measurements (references are shown in Table 1) for surface heat loss.

Champagne Pool and Kerosene Creek have the highest heat flow discharge within the field, in the WWR-2 model, of 20 MW and 25 MW respectively. In the southern areas, Reporoa and Golden Springs-Butcher's Pool can be combined as one system producing a total of 51.5 MW, close the observed data of 50 MW. The surface heat flow map is presented in Figure 11.

Table 3. Summary of heat flow comparison

Field	Measured (MW)	WWR-1 (MW)	WWR-2 (MW)
Waiotapu	581	487	579
Waikite	50	56	55
Reporoa	36	44	47
Golden Springs-Butcher's Pool	14	4	4.5
Total	681	591	685.5

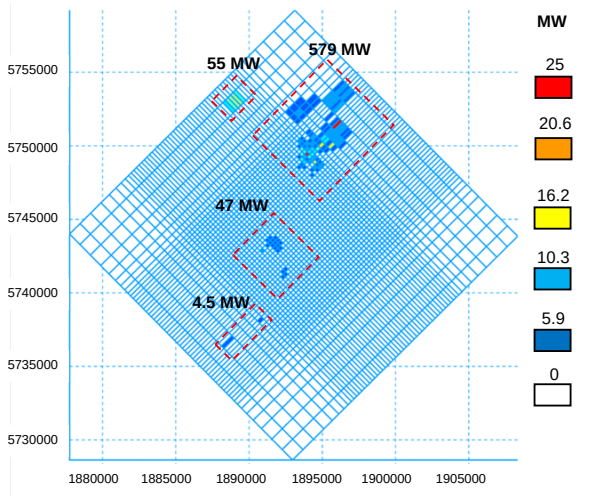

Figure 11. Areal view of surface heat flow of model WWR-2

6.2 Temperature profiles

Inclusion of surface heat discharges from Maungaongaonga and Maungakakaramea disrupted the steady state temperature matches, obtained in WWR-1. To improve the match of the model WWR-2 and measured downhole data, many different runs were tried by adjusting permeabilities and location and magnitude of heat sources (Figure 11). The best-fit temperature profiles are shown in Figure 12.

According to the model and based on actual measurements, temperature profiles in wells WT1, WT2 and WT3 suggest a shallow, thermal inversion zone (Figure 12). The temperature inversions indicate occurrence of lateral flow. Shallow cold flows are derived by advective, terrain-induced inflows of infiltrating surface waters mixing with the upflowing thermal water (Kaya *et al.*, 2015).

Temperature inversions are also caused by an abundance of jointing in the Waiotapu Ignimbrite, which gives high horizontal permeability to allow colder fluids to flow laterally into the field (Wood, 1994). The uplifted Paeroa Block in the northwest and the Kaingaroa Ignimbrite in the east (Figure 9) provide cold ground water inflows. For the Reporoa area, the RP1 temperature profile suggests that cold water inflow is located between approximately 100 mRL to -300 mRL. These flows are represented in the model by assigning a preferentially high horizontal permeability to the flow regions.

The effects of these cold inflows are not very strong in central Waiotapu wells (WT4, WT6 and WT7) due to their proximity to a strong upflow zone (Figure 12).

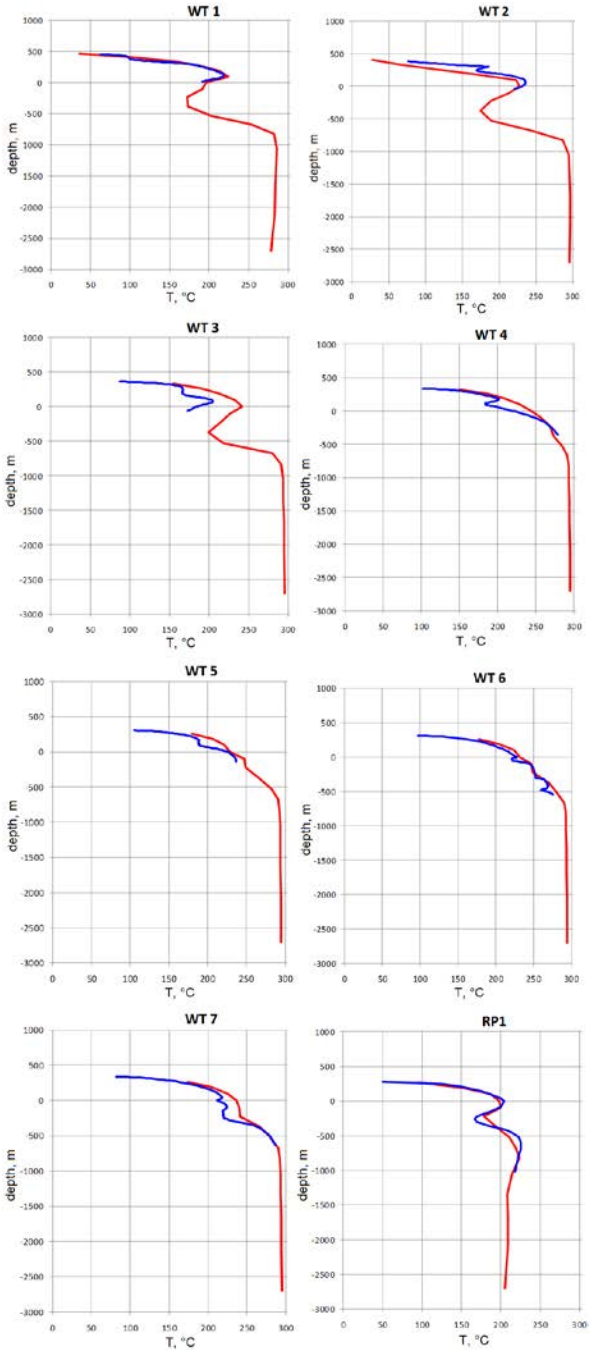

Figure 12. Temperature vs depth for Waiotapu and Reporoa wells, field data (blue) and model results (red)

6.3 Chloride concentration

NaCl discharge to the surface is calculated by considering the NaCl concentration from the spring wells and flows from the uppermost model layer. Areal distribution of surface NaCl concentration for model WWR-2 is shown in Figure 13. Since field measurements are in Cl concentration, in order to convert model results to represent NaCl content, Cl concentration was assumed to be ~61% of the NaCl fraction.

Table 4 explains that areas within Waiotapu show a good match for Cl concentration values. The Reporoa area shows a slightly lower Cl value at the surface, and this can be attributed to a southerly cold inflow from a shallow zone as suggested by Kaya *et al.* (2014) and Newson (1993). However, the Waikite area shows a higher Cl concentration. Stewart (1994) emphasized that in Waikite a constant ratio between chloride and bicarbonate concentration suggests that mixing takes place at depth before boiling occurs. According to Giggenbach and Stewart (1982), bicarbonate is formed by the reaction of dissolved CO_2 with rock as a result of cooling by dilution with groundwater. However, since fluid-rock interactions are not considered for this modelling study, it is not possible to observe this effect in WWR-2.

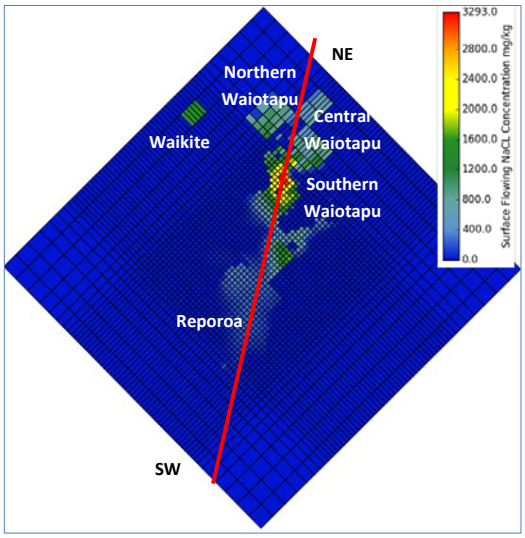

Figure 13. WWR-2 model NaCl distribution

Table 4. Chloride concentration comparison

	Field Cl conc. (mg/kg)*	WWR-2 Model		
		NaCl conc. (mg/kg)	Cl conc. (mg/kg)	Model Cl fraction (%)
Northern Waiotapu	525	900	549	0.055
Central Waiotapu	1049	1600	976	0.098
Southern Waiotapu	1979	3293	2009	0.201
Reporoa	458	800	488	0.049
Waikite	140	900	549	0.055

*Data from Giggenbach *et al.* (1994)

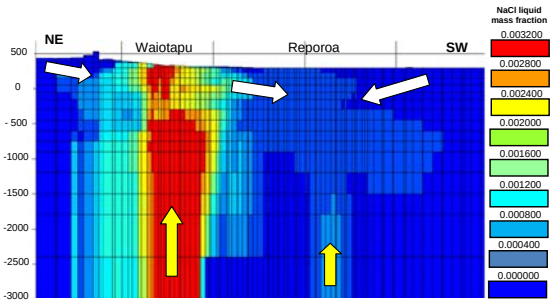

Figure 14. NaCl distribution along NE-SW

According to Figure 14 and Figure 15 the NaCl liquid mass fraction and temperature profile is coherent with the main upflow zone at Waiotapu. These figures also agree with Giggenbach et al. (1994), which indicates that secondary upflow from beneath Reporoa is associated with mixing and dilution of southern intermediate Cl waters from Lake Ngakoro and low Cl condensate.

The NE-SW cross-section in Figure 16 also indicates boiling in the Waiotapu reservoir. Boiling takes place at a shallow depth of -400 mRL (Cl of ~1700 mg/kg and 240 ^{o}C), and this is slightly consistent with the value Cl of ~1350 mg/kg and 230 ^{o}C as suggested by Hedenquist (1991). This boiling also causes an increase in Cl concentration (as observed in Figure 14). However since the atmosphere of the model includes a high NCG content, it is difficult to distinguish between vapour saturation distribution and an unsaturated zone above water table.

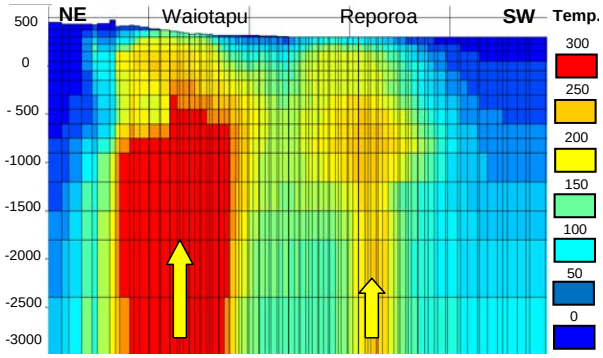

Figure 15. Temperature (°C) distribution along NE-SW

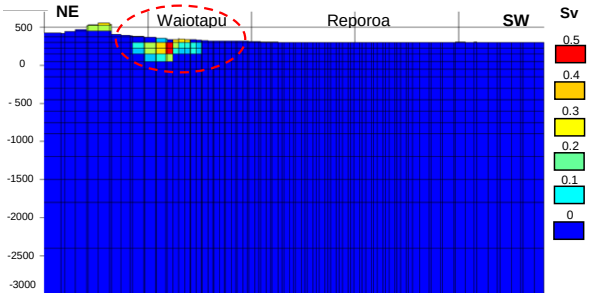

Figure 16. Vapour saturation distribution along NE-SW

Heat discharge to the surface is also calculated by using the chloride flux method, which is based on the enthalpy and chloride fraction obtained from the model. A summary of Cl fraction obtained from the model is given in Table 4. By using a similar method of Q/Cl to the one carried out by Smith (2013), the WWR-2 model resulted in a Cl flow of 244 g/s and Cl heat flow of 259 MW. This is compatible with Smith (2013), that estimates the heat outputs of the main Waiotapu field as between 250 and 300 MW.

7. CONCLUSIONS

In this paper, a water-salt-gas (EWASG) model of the Waiotapu, Waikite and Reporoa hydrothermal systems is presented. Inclusion of heat discharge from Maungaongaonga and Maungakakaramea domes and representation of vadose zones and infiltration regions required further calibration for the temperature profiles and surface heat discharges. The calibration has resulted in a generally good match in temperature profiles and total heat discharge, from each field. The numerical model also showed compatible results with measured chloride data.

The WWR-2 model quantifies a total heat loss of ~685 MW by using an anomalous heat flow calculation and estimates 259 MW heat discharge by using 244 gr/s of Cl fraction, which was derived from the model. The best maximum Cl fraction distributions across the model, which includes northern Waiotapu, central Waiotapu, southern Waiotapu, Reporoa and Waikite, are 0.05%, 0.09%, 0.2%, 0.049% and 0.055% respectively. The model also confirms boiling and dilution in shallow parts of Waiotapu, with an average Cl of ~1700 mg and reservoir temperature of approximately 240 °C.

For a more accurate representation this study could be extended by further work, including a representation of the system with a non-isothermal reactive geochemical transport module, which includes a capability for modelling chemical reactions between the liquid, gaseous and solid phases.

ACKNOWLEDGEMENTS

The authors would like to appreciate Angus Yeh for updating TIM in order to enable the visualization of normalised chloride concentration.

REFERENCES

Battistelli, A., Calore, C., & Pruess, K. (1997). The simulator TOUGH2/EWASG for modelling geothermal reservoirs with brines and non-condensible gas. *Geothermics*, *26*(4), 437-464.

Benseman, R. F., Fisher, R. G., & Dickinson, D. J. (1963). Survey of Surface Heat Output at Waiotapu *DSIR Bulletin* (Vol. 55, pp. 50-58).

Bibby, H. M., Bennie, S. L., Stagpoole, V. M., & Caldwell, T. G. (1994). Resistivity structure of the Waimangu, Waiotapu, Waikite and Reporoa geothermal areas, New Zealand. *Geothermics*, *23*(5–6), 445-471.

Bignall, G. (1990). *Hydrology and Hydrothermal Alteration, Reporoa Well (1), Reporoa, New Zealand*. Proceedings 12th New Zealand Geothermal Workshop.

Geothermics. (1994). *Volume 23*(Geothermics Issues 5–6).

Giggenbach, W., Sheppard, D. S., Robinson, B. W., Stewart, M. K., & Lyon, G. L. (1994). Geochemical structure and position of the Waiotapu geothermal field, New Zealand. *Geothermics*, *23*(5–6), 599-644.

Giggenbach, W., & Stewart, M. (1982). Processes controlling the isotopic composition of steam and water discharges from steam vents and steam-heated pools in geothermal areas. *Geothermics*, *11*(2), 71-80.

Glover, R. B., Klyen, L. E., & Crump, M. E. (1992). *Spring Chemistry of the Waikite-Puakohurea Thermal Area.* Proceedings: 14th New Zealand Geothermal Workshop, New Zealand.

Grindley, G. W., Mumme, T. C., & Kohn, B. P. (1994). Stratigraphy, paleomagnetism, geochronology and structure of silicic volcanic rocks, Waiotapu/Paeroa range area, New Zealand. *Geothermics*, *23*(5–6), 473-499.

Healy, J., & Hochstein, M. (1973). Horizontal flow in hydrothermal systems. *J. Hydrol. NZ*, *12*, 71-82.

Hedenquist, J. W. (1991). Boiling and dilution in the shallow portion of the Waiotapu geothermal system, New Zealand. *Geochimica et Cosmochimica Acta*, *55*(10), 2753-2765.

Hedenquist, J. W., & Browne, P. R. L. (1989). The evolution of the Waiotapu geothermal system, New Zealand, based on the chemical and isotopic composition of its fluids, minerals and rocks. *Geochimica et Cosmochimica Acta*, *53*(9), 2235-2257.

Hochstein, M. P. (2007). Changes in geothermal manifestations and other surface features since the start of the thermal exploitation of the; Mokai and Rotokawa Geothermal Fields, and an assessment of the Tokaanu-Waihi-Hipaua, Te Kopia and Reporoa Geothermal Fields and their Regional Plan Classification *Technical Report Series 27* (pp. 91).

Hochstein, M. P., & Browne, P. R. L. (2000). Surface manifestations of geothermal systems with volcanic heat sources. *Encyclopedia of volcanoes*, 835-855.

http://www.linz.govt.nz/topography/topo-maps/

Kaya, E., O'Sullivan, M. J., & Hochstein, M. P. (2014). A three dimensional numerical model of the Waiotapu, Waikite and Reporoa geothermal areas, New Zealand. *Journal of Volcanology and Geothermal Research 283*, 127-142.

Kaya, E., O'Sullivan, M. J., & Hochstein, M. P. (2015). *Aspects of Natural Heat Transfer of Geothermal System in Moderate Terrain: the Greater Waiotapu Geothermal System.* Proceedings: World Geothermal Congress 2015, Melbourne, Australia.

Littler, C., Crawford, N., Cowie, N., Hill, R. (2012). Geothermal Features Annual Monitoring Report *Environment Waikato technical report 2013/10.*

Lynne, B. Y. (2009). Monitoring of Geothermal Features *Environment Waikato Technical Report 2009/25.*

Nairn, I., Wood, C., & Bailey, R. (1994). The Reporoa Caldera, Taupo Volcanic Zone: source of the Kaingaroa Ignimbrites. *Bulletin of Volcanology*, *56*(6), 529-537. doi: 10.1007/BF00302833

Newson, J. (1993). *Geothermal and groundwater hydrology of the Reporoa-Waiotapu Basin.* (MSc), University of Auckland, Auckland, New Zealand.

Newson, J. (2010). Geothermal Features Annual Monitoring Report, June 2010 (pp. 50-54).

O'Sullivan, M. J., & Bullivant, D. P. (1995). *A graphical interface for the TOUGH family of flow simulators', Proc. TOUGH Workshop '95, Berkeley,California*.

O'Sullivan, J., Croucher, A., Yeh, A., & O'Sullivan, M. J. (2013). *Improver Convergence for Air-Water and CO2-Water TOUGH2 Simulations*. Proceedings 35th New Zealand Geothermal Conference, New Zealand.

Pope, J., & Brown, K. (2014). Geochemistry of discharge at Waiotapu geothermal area, New Zealand–Trace elements and temporal changes. *Geothermics*, *51*, 253-269.

Pruess, K., Oldenburg, C., & Moridis, G. (1999). *TOUGH2 User's Guide, Version 2.0 Berkeley, California: Lawrence Berkeley National Laboratory, Earth Sciences Division.*

Risk, G. F., Caldwell, T. G., & Bibby, H. M. (1994). Deep resistivity surveys in the Waiotapu-Waikite-Reporoa region, New Zealand. *Geothermics*, *23*(5–6), 423-443.

Smith, G. J. (2013). Waiotapu Heat Flux 2013. In F. G. Project (Ed.), (pp. 71): Geothermal Scientific Investigation, Ltd.

Sorey, M., & Colvard, E. M. (1994). *Measurements of heat and mass flow from thermal areas in Lassen Volcanic National Park, California, 1984-93*: US Geological Survey.

Stewart, M. (1994). Groundwater contributions to Waikite geothermal fluids. *Proceedings 16th Geothermal Workshop*, 109-114.

Wellmann, F. J., Croucher, A., & Regenauer-Lieb, K. (2012). Python scripting libraries for subsurface fluid and heat flow simulations with TOUGH2 and SHEMAT. *Computers & Geosciences*, *43*(0), 197-206.

Wildland Consultants. (2001). Reporoa Geothermal Features. Contract Report No. 2348.

Wood, C. P. (1994). Aspects of the geology of Waimangu, Waiotapu, Waikite and Reporoa geothermal systems, Taupo Volcanic Zone, New Zealand. *Geothermics*, *23*(5–6), 401-421.

Yeh, A., Croucher, A.E., O'Sullivan,M.J., 2012. Recent developments in the AUTOUGH2 simulator. Proceedings: of the TOUGH Symposium 2012, Lawrence Berkeley National Laboratory, Berkeley, California.

Yeh, A., Croucher, A. E., & O'Sullivan, M. J. (2013). *TIM–Yet Another Graphical Tool for TOUGH2 Simulators*. Proceedings 35th New Zealand Geothermal Workshop, New Zealand.